



OPEN

An Integrated Microfluidic Chip System for Single-Cell Secretion Profiling of Rare Circulating Tumor Cells

SUBJECT AREAS:

LAB-ON-A-CHIP

CANCER

CANCER SCREENING

DIAGNOSTIC MARKERS

Yuliang Deng^{1*}, Yu Zhang^{1*}, Shuai Sun¹, Zihua Wang¹, Minjiao Wang¹, Beiqin Yu⁵, Daniel M. Czajkowsky^{3,4}, Bingya Liu^{1,5}, Yan Li⁶, Wei Wei⁷ & Qihui Shi^{1,2,3,4}Received
20 October 2014Accepted
27 November 2014Published
16 December 2014

Correspondence and requests for materials should be addressed to Q.H.S. (qihuishi@sjtu.edu.cn)

* These authors contributed equally to this work.

¹Key Laboratory of Systems Biomedicine (Ministry of Education), Shanghai Jiao Tong University, Shanghai, China, ²State Key Laboratory of Oncogenes and Related Genes, Shanghai Jiao Tong University, Shanghai, China, ³Center for Bio-Detection and Bio-Instrumentation, Shanghai Jiao Tong University, Shanghai, China, ⁴School of Biomedical Engineering, Shanghai Jiao Tong University, Shanghai, China, ⁵Ruijin Hospital, School of Medicine, Shanghai Jiao Tong University, Shanghai, China, ⁶Shanghai Municipal Hospital of Traditional Chinese Medicine, Shanghai, China, ⁷Department of Molecular and Medical Pharmacology, David Geffen School of Medicine, University of California, Los Angeles, CA, USA.

Genetic and transcriptional profiling, as well as surface marker identification of single circulating tumor cells (CTCs) have been demonstrated. However, quantitatively profiling of functional proteins at single CTC resolution has not yet been achieved, owing to the limited purity of the isolated CTC populations and a lack of single-cell proteomic approaches to handle and analyze rare CTCs. Here, we develop an integrated microfluidic system specifically designed for streamlining isolation, purification and single-cell secretomic profiling of CTCs from whole blood. Key to this platform is the use of photocleavable ssDNA-encoded antibody conjugates to enable a highly purified CTC population with <75 'contaminated' blood cells. An enhanced poly-L-lysine barcode pattern is created on the single-cell barcode chip for efficient capture rare CTC cells in microchambers for subsequent secreted protein profiling. This system was extensively evaluated and optimized with EpCAM-positive HCT116 cells seeded into whole blood. Patient blood samples were employed to assess the utility of the system for isolation, purification and single-cell secretion profiling of CTCs. The CTCs present in patient blood samples exhibit highly heterogeneous secretion profile of IL-8 and VEGF. The numbers of secreting CTCs are found not in accordance with CTC enumeration based on immunostaining in the parallel experiments.

Circulating tumor cells (CTCs) are rare tumor cells (~1–100 CTCs per 10⁹ blood cells) shed from primary and metastatic tumor sites^{1,2}. They are generally believed to be the main source of cancer metastasis³, and their presence in the blood correlates with increased metastatic burden and a decrease time to relapse⁴. As a result, these cells are widely considered as one of the most promising biomarkers for hematogenous metastases, and tremendous effort has been directed toward exploring their diagnostic and prognostic potential^{1,2}. However, the metastatic propensity of CTCs has not been found to have clear correlations with the CTC enumeration and the molecular signature of their genome and transcriptome, presumably due to the extensive epigenetic and functional heterogeneity of CTCs. A large fraction of CTCs from cancer patients have been found to be, in fact, apoptotic^{5,6}, and only a small subset of CTCs exhibit a high propensity to seed distant metastases, although they may originate from the same lesion and have almost identical genetic profile^{2,7–9}. Therefore, functional proteins – those hyperactivated proteins in cancer cells with functional consequences – must be characterized at single cell resolution for each individual CTC to identify those with high viability and propensity for metastases.

A vast array of technologies has emerged to isolate and characterize CTCs. Most of them focus on the enumeration, the detection of genetic aberrations, and the identification of cell surface markers^{1,2,5–17}. Recently, genetic and transcriptional profiling of isolated single CTCs has been reported^{18–21}. However, techniques for quantitatively profiling the actual executors of cellular function – functional proteins (e.g., secreted protein, phosphoproteins) – at a single CTC resolution have not yet been achieved, owing to the limited purity of isolated CTC population generated by existing technologies and a lack of single-cell approaches that can handle a very low number of target cells to analyze rare and heterogeneous CTCs^{1,2,13–15,17}. Our goal is to develop a platform for quantitatively measuring secreted proteins from extraordinarily rare CTCs at single-cell levels. Secreted proteins including cytokines, chemokines, and growth factors play an important role in tumor cell metastasis



by promoting tumor cell proliferation, adhesion, migration and angiogenesis²². For example, recent work has demonstrated that entrapped melanoma CTCs in the lungs secrete high levels of the interleukin-8 (IL-8) to attract neutrophils and thus facilitate trans-endothelial migration and metastasis development²³. Analyzing secretomic profiles of single CTCs is particularly interesting for evaluating their viability, functional states and heterogeneity. Although ELISPOT assays have been employed to detect secreted proteins for counting viable CTCs, they are not quantitative measurements for secreted proteins, and the number of secreted proteins detected is very limited (one or two)²⁴.

To enable quantitative, single-cell secretomic profiling of rare CTCs, we developed an integrated microfluidic system that offers efficient isolation and single-cell functional characterization of rare CTCs from whole blood samples. Briefly, CTCs are first captured via photocleavable ssDNA-encoded antibody conjugates and microvortex-generating microfluidic chips. Captured CTCs are then photochemically released from the chip by brief UV irradiation, followed by sequential negative depletion of red blood cells (RBCs) and white blood cells (WBCs). High-purity CTCs are then transported to a single-cell barcode chip (SCBC) integrated with an enhanced poly-L-lysine (PLL) barcode pattern that enables capturing very low number of target cells on the chip. Individual CTCs are isolated in miniature chambers for profiling a panel of functional proteins secreted from single CTCs. In this study, we evaluated our platform using EpCAM-positive HCT116 cells (colorectal cancer cell lines) seeded into whole blood from healthy donors as a model system. Our microfluidic system is capable of processing 1 mL of whole blood sample in <2 hours with >70% isolation efficiencies and <75 'contamination' blood cells, leading to a high recovery of rare cancer cells with extremely low contaminated cells. In particular, this platform also enables sorting CTCs into specific phenotypes by surface marker signatures and performing single-cell secretomic profiling on these subsets.

Although this platform combines an array of previously reported chip technologies, two material modifications are vital in the realization of streamlined CTC capture, purification and single-cell detection of secreted proteins. First, photocleavable ssDNA-encoded antibody conjugates are synthesized for high-efficient CTC capture-and-release without impairing cell viability, which enables subsequent purification to retrieve a pure CTC population for downstream functional analysis. Second, PLL barcode patterning

created on SCBC permits efficiently recapturing single CTCs into each microchamber from a large volume of working solution that contains a very low number of purified CTCs for single-cell secretomic profiling. Overall, each working chip has been iteratively optimized to be adapted to our integrated microfluidic platform for streamlined isolation, purification and functional analysis of extraordinarily rare target cells from complex biological samples.

Results

Integrated microfluidic system and strategy. The overall strategy for CTC isolation and single-cell analysis are depicted in Fig. 1 and Fig. S1. Fig. S2 shows the experimental set-up and microfluidic chips used in the system. High-efficient CTC capture from the whole blood is achieved by ssDNA-encoded antibody conjugates and microvortex-generating herringbone chips^{10–12} with immobilization of complimentary ssDNA. After on-chip cell capture, a mixture of CD45 (common leukocyte antigen) and CD15 (granulocyte marker)-coated immunomagnetic beads are introduced in the chip and incubated with non-specifically bound WBCs. Importantly, the ssDNA-encoded antibody conjugate contains a photocleavable moiety that enables photochemical release of intact captured CTCs from the surface by briefly exposing to UV irradiation. To achieve high-purity CTC population for single-cell analysis, a two-step purification is employed to remove 'contaminated' RBCs and WBCs in the released CTC population. Spiral chip described before^{13–15} rapidly removes RBCs by size-based separation and retains all nucleated cells (CTCs and WBCs). RBC-depleted cells are flowed through a microfluidic chip closely above arrayed magnets to remove WBCs that are bound with magnetic beads¹⁶. Finally, retrieved CTCs are transported to a SCBC with PLL barcode patterning for detection of secreted proteins from single CTCs.

SCBC is the technology workhorse for single-cell functional proteomics assay to measure the quantity and functional state (e.g., phosphorylation) of a panel of secreted or intracellular signaling proteins across many otherwise identical cells, as shown in Fig. S3^{25–28}. However, a fundamental limitation of this device is the absolute requirement of a sufficiently high initial concentration of cells (usually, ~1,000 cells/ μ l). With this concentration, the random distribution of cells in the 2720 microchambers of SCBC, results in single cells in ~25% of microchambers, which is sufficient for robust single-cell analysis. As for extraordinarily rare CTCs, the absolute

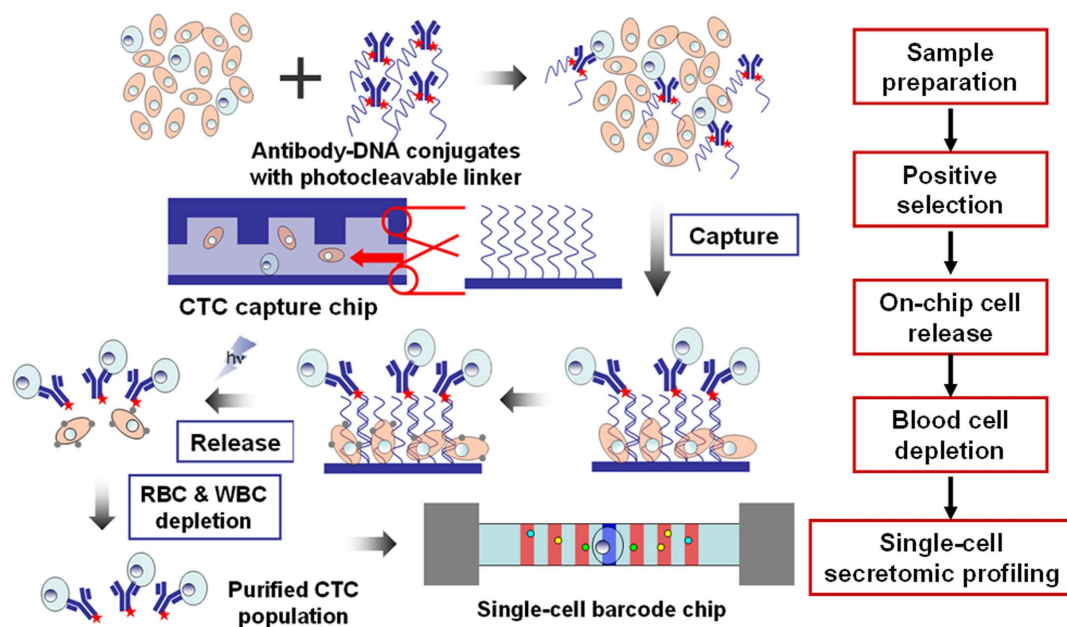


Figure 1 | Overall strategy for CTC isolation and single-cell secretomic analysis.

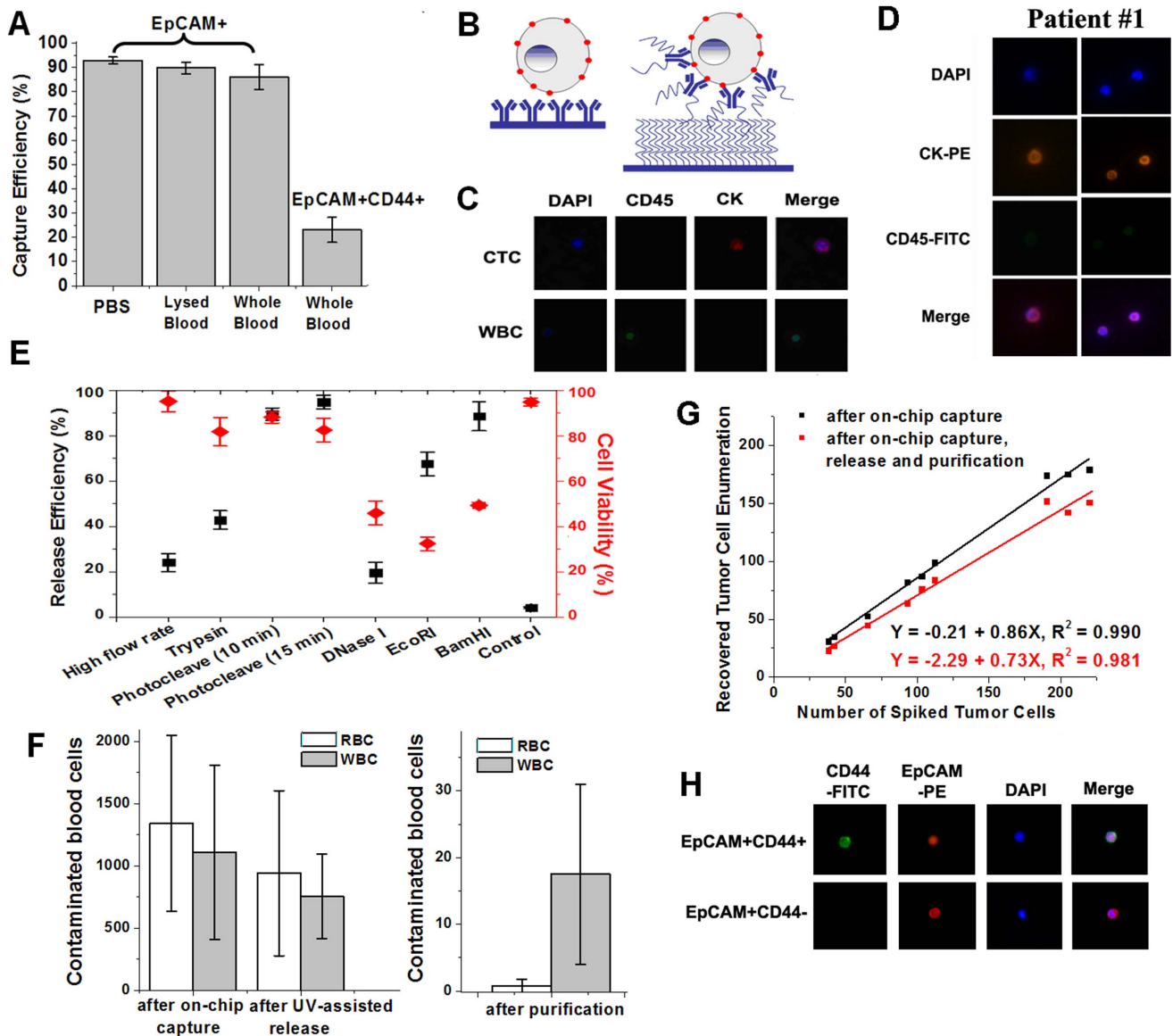


Figure 2 | Efficiencies of on-chip target cell capture, release, and purification. (A) Cell-capture efficiencies of ~200 EpCAM-positive HCT116 cells spiked in 1.0-ml of PBS, lysed blood and whole blood by herringbone chips at the flow rate of 1 mL/h. Error bars show standard deviations ($n=3$). (B) Generic concept of on-chip cell capture strategies. (C) Three-color immunocytochemistry method based on PE-labeled anti-pan-CK, FITC-labeled anti-CD45, and DAPI nuclear staining was applied to identify and enumerate CTCs from whole blood after on-chip cell capture. (D) Representative images of isolated CTCs from lung cancer patient #1's blood sample stained with antibodies against cytokeratin (red), CD 45 (green) and DAPI (blue). (E) On-chip release efficiency and cell viability by various releasing approaches. (F) Numbers of RBCs and WBCs non-specifically bound on the herringbone chip after on-chip capture, released together with HCT116 cells after UV irradiation, and after two-step purification to deplete blood cells. (G) Cell recovery under different number of spiked tumor cells as inputs. (H) Three-color immunocytochemistry method based on PE-labeled EpCAM, FITC-labeled CD44 and DAPI nuclear staining was applied to identify EpCAM⁺CD44⁺ and EpCAM⁺CD44⁻ cells.

number and the concentration of CTCs are substantially lower (0.1–1 cell/ μ l) than SCBC's requirement. Thus, the current SCBC technology causes significant loss of target cells, and cannot possibly be used for subsequent analysis. For this reason, an efficient on-chip cell capture capability is greatly needed for retaining rare target cells on SCBC, for which the enhanced PLL barcode patterning was designed.

CTC capture efficiency and enumeration in patient samples. To evaluate the efficiency of our system, we spiked EpCAM-positive HCT116 cells²⁹ into healthy whole blood as the model system. Pre-stained HCT116 cells were spiked into PBS, lysed blood (whole blood with lysis of RBCs) and whole blood from healthy donors to generate cell suspensions at 200 cells/mL. 1.0 mL of cell suspension was mixed with anti-EpCAM-PC-M' conjugate for 25 min (PC: photocleavable

linker, M': ssDNA, Fig. S4), and unbound conjugates and plasma proteins were then discarded by centrifuging, followed by re-suspending cell pellet in PBS containing 0.1% BSA to generate a 2.0 mL of cell suspension. The cell suspension was then processed with four herringbone chips operated in a parallel-serial (2P2S) configuration at an optimized flow rate of 1 mL/h. Each chip had a 200 μ m-microchannel with high-density ssDNA (M) immobilization (Fig. S5). Pre-stained tumor cells were then imaged and counted using a fluorescence microscope.

Fig. 2A shows high CTC recovery based on our protocol under different conditions. HCT116 cells spiked in PBS reaches a ~93% recovery, which is calculated based on counting pre-stained CTCs on the herringbone chips and in the waste (Fig. S6–S8). The cell loss may be due to those HCT116 cells with low expression of EpCAM.



Spiking in lysed blood reaches a reduced $\sim 89\%$ recovery due to a large number of surrounding WBCs and a high-rate post-capture rinse (5 mL/h, 5 min) for washing off non-specific bound blood cells. A capture efficiency of $\sim 86\%$ is achieved when spiking in whole blood. Minimal cell loss of our method promises applications for processing clinically-relevant blood samples. Notably, in previous antibody-based CTC capture approaches^{10–12}, cell capture is driven by surface-immobilized antibody to cell surface marker interactions (heterogeneous cell capture). However, in this study, CTCs are captured firstly by free ssDNA-antibody conjugates in the solution phase (homogeneous cell capture), and then by the increased avidity of the multivalent conjugates for the complementary DNA strands on the microarray through cooperative binding (Fig. 2B). Previous studies^{30,31} demonstrated that this homogeneous method exhibited higher cell capture efficiency than the heterogeneous method. This is owing to a greater range of orientations the antibodies may adopt in solution compared to the much more limited range when they are immobilized on the surface, which ultimately results in an enhanced binding between conjugates and cell surface marker in solution.

After validation of the CTC capture device and protocol (Fig. 2C), we processed blood samples from metastatic lung cancer patients. A 4-mL blood sample was taken from patients for CTC enumeration and single-cell secretion profiling (see Supplementary Methods). 2 mL of blood sample was firstly centrifuged to remove plasma, followed by mixing with ssDNA-antibody conjugates and on-chip CTC capture. CTCs were enumerated based on CK-positive, CD 45 negative and DAPI positive criteria. Based on this classification, putative CTCs were successfully detected in all lung cancer patients, ranging from 10 to 35 CTCs in 2mL of whole blood (Table 1 and Fig. 2D), while healthy subjects had negligible CTCs count (0–1) (Fig. S9, Table S2). In a parallel experiment, the other 2 mL blood sample was processed with the system for CTC capture, purification and single-cell detection of secreted proteins.

CTC release efficiency. Intact release of captured CTCs without harsh conditions is critical for downstream molecular and functional analysis, which is technically challenging due to strong cell binding to the antibody-functionalized surfaces³². In previous studies, cell release was achieved by trypsinization that degrades all cell surface proteins³³, a high flow rate combined with trypsinization that yields a $\sim 60\%$ release³⁴, a chemically grafted thermosensitive polymer network on silicon nanowire substrates that is very labor-intensive³⁵, and an aptamer-based capture in where released is mediated by nuclease³⁶. In this study, we integrate a photocleavable moiety in the ssDNA-encoded antibody conjugates for cell release. To optimize the cell release efficiency and viability, we investigated various release methods, including high fluid shear stress, trypsinization, and digestion of DNA by deoxyribonuclease or restriction endonuclease. The release efficiency is defined as the ratio of the number of cells released to the number of cells captured. Viability of released cells is measured to in the meantime (Fig. S10). As shown in Fig. 2E, a release efficiency of $\sim 90\%$ is achieved after 10 min of photoirradiation (365 nm, 1.2 mW/cm²)

with a cell viability of $\sim 88\%$ (Fig. S11). A 15 min photoirradiation increases cell recovery to $\sim 95\%$, while viability of released cells is decreased to $\sim 82\%$. Compared with other methods such as high flow rate washing, trypsinization, DNase I and restriction endonuclease (EcoRI, BamHI) treatment, photochemical release is an optimal method for its simple and efficient release mechanism, limited cell death, one-step chemistry to synthesize photocleavable conjugates, and no interference with downstream analysis by this reagent-free method^{37,38}.

Purity of isolated CTC population. After on-chip CTC capture, a 5 mL/h post-capture rinse is used to wash off non-specifically bound blood cells on the herringbone chips. Among separate studies, we found that there were 432–2050 WBCs (mean 1109) and 513–2100 RBCs (mean 1342) on the selection surface of the chips (200 mm long and 1.0 mm wide), as shown in Fig. 2F. A mixture of CD 45 and CD 15-coated immunomagnetic beads are then introduced in the microchannels and incubated with non-specifically bound WBCs. Following photoirradiation and high-rate flow, blood cells non-specifically bound on the selection surface are released with photocleaved CTCs simultaneously. 754 WBCs (range 368–1151) and 940 RBCs (range 128–1680) were found released with CTCs (Fig. 2F). For purification, released cells are firstly transported to a spiral chip for RBC isolation at an optimized flow rate of 12 mL/h (Fig. S12, S13), and then flowed through microfluidic channels sitting on a set of magnets for depletion of WBCs (Fig. S14)¹⁶. After blood cell depletion, released blood cells from each herringbone chip were reduced to ~ 18 WBCs (range 4–36) and ~ 1 RBC (range 0–2) and CTC recovery of release and purification was determined to be $\sim 84\%$ (Fig. 2G). The total recovery of spiked HCT116 cells from whole blood reached closed to 72% (Fig. 2G and Fig. S15), and total ‘contamination’ blood cells were lower than 75 because four herringbone chips were used for CTC isolation. This degree of CTC cell purity is ~ 5 –20 fold better than that obtainable with present devices^{13–15,17}, suitable for further functional proteomic analysis. In addition, this two-step purification procedure doesn’t need costly materials and sophisticate fabrication^{39,40}.

Selection of phenotypic subset of CTCs. Importantly, the photocleavable ssDNA-encoded antibody-based strategy allows for selection of a subset of CTCs with specific phenotypes defined by a combination of cell surface markers. In colorectal cancer, EpCAM^{high}CD44⁺ cell were suggested as cancer stem cell phenotype⁴¹. To select EpCAM⁺CD44⁺ tumor cells from whole blood samples (Fig. S16), we firstly incubate anti-EpCAM-PC-M’ conjugate with whole blood, and then process with M-immobilized herringbone chips to capture EpCAM⁺ cells. Upon photochemical release of EpCAM⁺ cells, EpCAM⁺CD44⁺ cells are captured on a new herringbone chip with pre-coating of anti-CD44-PC-L’ conjugates at a total recovery of $\sim 23\%$ (Fig. 2A, 2H), which can be further photochemically released. EpCAM⁺CD44⁺ cells in the solution reach a recovery of $\sim 48\%$. As a result, our platform provides a powerful tool in isolating specific phenotypic subsets of

Table 1 | Clinico-pathological characteristics and CTC enumeration of metastatic lung cancer patients. Total CTC number is enumerated in 2 mL of patient’s blood sample based on DAPI+/CK+/CD 45- criteria. Secreting CTCs refer to isolated and purified CTCs with VEGF secretion in another 2 mL blood sample taken from the same patient. (SCC: Small cell carcinoma; *One microchamber contains two cells and we count as one secreting cell.)

Patient #	Age	Sex	Histology	Cancer Stage	Receiving Treatment	CTC no./2 mL	
						Total CTC no.	Secreting CTC no.
1	68	M	SCC	IV	Yes	28	5
2	79	M	SCC	IIIB	Yes	26	8
3	60	F	SCC	IV	Yes	10	2*
4	70	M	SCC	IV	Yes	35	12

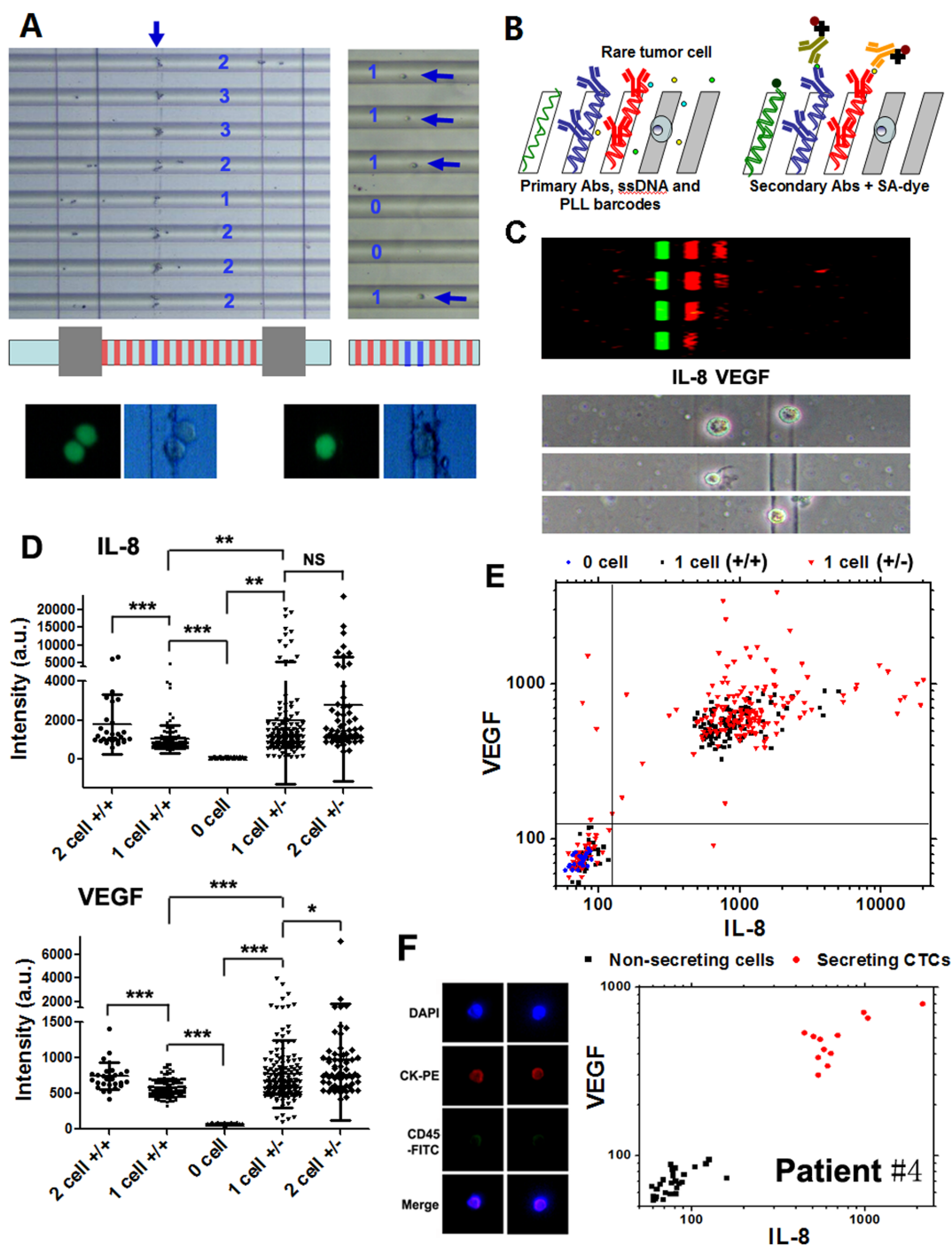


Figure 3 | Single-cell secretomic data of isolated CTCs. (A) On-chip cell capture by PLL barcode patterns located in microchambers of SCBC. Top left, ~50,000 cells added as input and captured by single 20 μm -wide PLL stripe. Top right, ~500 cells added as input and captured by double 20 μm -wide PLL stripes. Each microchamber is labeled with numbers that reflect the number of cells captured in the microchamber. Bottom, viable tumor cells captured by PLL barcode pattern on the SCBC show green fluorescence after staining with calcein AM. (B) Drawing of the ssDNA-encoded primary antibody and PLL barcode array used for capture of rare tumor cells and secreted proteins from single- or few-cells, and then developed for the detection of those proteins. SA: streptavidin. (C) Top, representative scanned images of barcode signals from single-cell chambers of EpCAM⁺CD44⁺ cells. Green bars represent location reference, and red bars are protein signals. Bottom, representative images of EpCAM⁺CD44⁺ cells captured by PLL barcode pattern in microchambers. (D) Scatter plots of assayed levels of IL-8 and VEGF for individual microchambers containing zero, one or two HCT116 cells (+/+ : EpCAM⁺CD44⁺ cells; +/- : EpCAM⁺CD44⁻ cells). Single- or two-cell microchambers with intensities of IL-8 and VEGF lower than 125 are attributed to dead tumor cells or ‘contaminated’ WBCs, and thus not displayed in the scatter plots. The averaged fluorescence intensity (y axis) with SD is overlaid for each protein. Statistical uniqueness is evaluated by two-tailed Student’s t-test assuming unequal variance (***P < 0.0001; **P < 0.005; *P < 0.05; NS, not significant). (E) Scatter plots of single-cell IL-8 versus VEGF derived from SCBC measurements on EpCAM⁺CD44⁺ cells and EpCAM⁺CD44⁻ cells. The gates separating cytokine or growth factor-secreting and nonsecreting cells are determined from 0 cell microchamber (background) measurements (blue). (F) Left, representative fluorescence images of isolated CTCs from patient #4’s blood sample (2 mL) stained with antibodies against cytokeratin (red), CD 45 (green) and DAPI (blue). Right, scatter plots of IL-8 versus VEGF derived from SCBC measurements on CTCs that were isolated and purified from patient #4’s another 2 mL blood sample.



rare cells, representing a unique advantage over other antibody-based CTC capture approaches.

Single-cell secretion profiling of isolated CTCs. After capture-and-release, purified CTCs are then transported to SCBC for single-cell secretomic analysis. SCBC contains 2720 microchambers, and each microchamber accommodates single or a defined number of cells. To avoid significant cell loss during the cell loading step, we developed an enhanced PLL coating ($M_w \geq 300,000$) in the format of barcode (20 μm wide) on the glass substrate with function of adhering rare target cells from the solution based on electrostatic interaction between polyanionic cell surfaces and the polycationic layer of immobilized polylysine (Fig. 3A). The height of microchannel is designed to be close to the size of cells, allowing sufficient contact with the PLL barcodes. In the experiment, we found the cell attachment took place as soon as the cells made contact with the surfaces of PLL barcodes. For a solution containing less than 1000 cells, the on-chip capture efficiency is found to be close to 55%. Meanwhile, staining PLL barcode-retained cells on SCBC exhibits $>80\%$ viability (Fig. 3A), demonstrating that isolated CTCs are not damaged during the cell purification process. After cell loading, the captured cells are cultured inside the microchambers for 6 h, followed by loading a detection antibody mixture and the fluorescent probes to complete the on-chip immunoassay (Fig. 3B). We assayed IL-8 and VEGF in this study because of their association with formation of metastases and poor prognosis in colorectal cancer^{42,43}.

As a proof-of-concept experiment, we spiked ~ 2000 HCT116 cells in 1 mL of whole blood as a model system. We isolated and purified EpCAM⁺CD44⁺ and EpCAM⁺CD44⁻ HCT116 cells from the whole blood, as described before, followed by secretomic profiling on a PLL-patterned SCBC (Fig. S17 and S18). We successfully assayed 140 single cells, 34 two-cell chambers from EpCAM⁺CD44⁺ cells, and 213 single cells, 76 two-cell chambers from EpCAM⁺CD44⁻ cells, as well as 25 representative zero-cell chambers after 6 h of on-chip culture (Fig. 3C). It's worthwhile to note that the number of proteins detected can be easily expanded to ~ 12 functional proteins as reported before¹⁴, given they are identified by spatial locations of the barcode rather than fluorescence colors. Secretomic data, when binned according to the numbers of cells per chamber, yield statistically distinct protein signals (Fig. 3D). Most notably, single-cell protein signals could be clearly detected, and there is also clear separation of secreting and non-secreting cells, as visualized by in Fig. 3E. We gated the fraction of cells detected to secrete a given protein using background signals from empty chambers. Single-cell analysis shows that 23.6% and 23.9% of single cells (Fig. 3E) are identified as non-secreting cells in EpCAM⁺CD44⁺ and EpCAM⁺CD44⁻ phenotypes, respectively, indicating dead tumor cells or contaminated WBCs. An estimated of 76% of single cells are found to secrete detectable VEGF, characteristic of viable tumor cells. The abundance of IL-8 and VEGF secreted from EpCAM⁺CD44⁻ cells, averaged over viable single cells, are greater than those from EpCAM⁺CD44⁺ cells, in agreement with measurements of these same proteins from cell culture supernatants (Fig. S19). Further biological studies are warranted to explain the higher expression levels of VEGF and IL-8 in EpCAM⁺CD44⁻ HCT116 cells. Coefficients of variation of IL-8 and VEGF levels from EpCAM⁺CD44⁻ cells are higher than those from EpCAM⁺CD44⁺ cells (Fig. S20), indicating greater functional heterogeneity in the EpCAM⁺CD44⁻ phenotype.

Patient sample measurement. Finally, single-cell secretomic analysis was conducted on CTCs isolated and purified from 2 mL of blood sample that was taken from metastatic lung cancer patients. For patient #4, we identified 39 cell-containing microchambers on the PLL barcode-patterned SCBC and 12 of them (all containing single cells) exhibited significant and heterogeneous signals of IL-8

and VEGF, characteristic of 12 viable and secreting CTCs detected on SCBC (Fig. 3F). The remaining 27 non-secreting cells were either CTCs that were not functional (dead cells or non-secreting cells) or contaminated WBCs. By contrast, in a separate experiment of CTC enumeration, 35 putative CTCs were identified in 2 mL of blood sample from the same patient based on the DAPI+/CK+/CD45-criteria (Table 1). 5, 10 and 2 secreting CTCs were identified in 2 mL of blood samples from patient #1, #2, and #3, respectively, and 28, 26, 10 putative CTCs were enumerated based on immunostaining in parallel experiments (Fig. S21).

Discussion

This study shows an integrated microfluidic system that permits isolation of rare CTCs or a specific phenotypic subset of those CTCs from whole blood samples with high recovery ($>70\%$) and high purity ($<75\%$ 'contamination' blood cells), and single-cell secretomic analysis of those isolated CTCs, resolving the functional states and the heterogeneity of CTCs. Different from previous investigations of CTCs that focuses on enumeration, the detection of genetic aberrations, and the identification of cell surface markers, secretomic profiles of CTCs represent a functional assessment because secreted proteins are found associated with formation of metastases and poor prognosis in cancer^{44,45}. Obviously, this system enables quantitative measurement of secreted proteins from extraordinarily rare CTCs in patients' blood samples with single-cell resolution.

Although this system consists of four previously reported microfluidic chips, two material modifications are vital in overcoming technical bottlenecks and therefore realize streamlined operation of CTC capture, purification and single-cell functional analysis. First, photocleavable ssDNA-antibody conjugates are utilized to achieve high-efficient CTC capture-and-release, enabling subsequent purification for retrieving a CTC population with high-purity. Second, an enhanced PLL barcode pattern is created to efficiently recapture those extraordinarily rare CTCs on SCBC from a large volume of working solution for subsequent single-cell secretomic analysis. Although a 55% of on-chip cell capture efficiency is not ideal, it represents a big improvement compared with the current SCBC technology that cannot analyze extraordinarily rare cells due to significant loss of target cells during the cell loading step.

We have shown this system can select phenotypic subsets of CTC population based on surface marker combination and identified different secretomic signatures of phenotypic subsets. This might help to uncover specific phenotypes associated high invasiveness and capability of generating metastases. More important, our system has successfully characterized the functional states and heterogeneity of CTCs that are present in the cancer patients' blood samples. These CTCs exhibit highly heterogeneous levels of secreted IL-8 and VEGF, and the numbers of secreting CTCs are found not in accordance with CTC enumeration based on immunostaining in the parallel experiments. Although only two secreted proteins (IL-8 and VEGF) were assayed to demonstrate the concept in this study, the number of proteins detected can be easily expanded to ~ 20 or more functional proteins as reported before²⁵⁻²⁸, delivering more critical and unique information associated with cancer metastasis and clinical prognosis. In spite of larger clinical studies that are warranted to further validate our approach and explore the clinical value of CTCs' secretomic profiles, our approach and system represent an advance in quantitative functional characterization of CTCs.

Additionally, the SCBC technology can also be used to monitor intracellular signaling pathways of CTCs. Previous studies have been limited by low protein recovery from rare CTCs⁴⁶. SCBC is able to measure the quantity and functional state (such as phosphorylation) of a panel of surface markers, intracellular signaling proteins and secreted proteins at the single-cell level²⁵⁻²⁸, and thus significantly enhances the information retrieved from CTC analyses.



Methods

Herringbone chip fabrication and modification. The herringbone microfluidic chips employed for rare cell capture were fabricated based on previous studies⁶. The patterned silicon mold was produced by a standard two-step photolithographic process. Each layer was 50 μm of negative photoresist SU8-2050 (MicroChem Corp., USA). The PDMS pre-polymer (Sylgard 184, Dow Corning, USA) was mixed in a ratio of 10:1, and subsequently casted on this lithographically patterned replicate. After curing at 80 °C for 2 h, the PDMS component was separated from the replicate, followed by trimming and hole introduction. To chemically modify the PDMS device, the microfluidic channels were treated with O₂ plasma (PDC-32G, Harrick Plasma, USA) to create silanol groups, followed by treatment of 4% (v/v) solution of (3-Aminopropyl)trimethoxysilane (Sigma-Aldrich, USA) in ethanol for 1 h at room temperature. Finally, the amine-group-modified PDMS chip was thermally bonded to a poly-L-Lysine (PLL) coated glass slide (Thermo Fisher Scientific Inc., USA). To immobilize DNA on the internal wall of the device, a mixture (1:1 v/v) of amine-modified DNA solution (300 μM, in DMSO) and 2 mM BS3 (in PBS, Thermo Scientific, USA) was filled into the device and flowed for 1.5 hours. The device was then stored in a sealed Petri dish with damp cotton for 1.5 hours, followed by washing with 0.02% SDS (in water) and deionized Millipore water. BS3 crosslinks amine-modified DNA with glass substrate and PDMS that are also modified with amine groups.

Single-cell barcode chip fabrication. The SCBC was assembled from a DNA barcode microarray glass slide and a PDMS slab containing a microfluidic circuit¹⁴. The PDMS microfluidic chip for the single-cell experiment was fabricated using a two-layer soft lithography approach. A push-down valve configuration was utilized with a thick control layer bonded to a thin flow layer underneath. The barcode-patterned glass slide was composed of DNA barcode for detection of secreted proteins and polylysine patterns for on-chip cell capture.

Fabrication of DNA and poly-L-lysine barcodes. The DNA and PLL barcode pattern was created with microchannel-guided flow patterning. The barcode patterning chips were fabricated based on previous studies¹⁴, containing a 20-microchannels array (20 μm in width and 30 μm in height). After bonding of PDMS device to the PLL-coated glass substrate, a library of DNA solutions (C, D, and M), diluted in a mixture of DMSO and deionized water (v/v=1:2) with a final concentration of 267 μM, as well as 0.2 w/v% PLL solution (Mw ≥ 300,000, Sigma-Aldrich) were flowed into each of the microfluidic channels. The solution-filled chip was placed in a desiccator to allow solvent to evaporate completely through the gas-permeable PDMS. Lastly, the PDMS elastomer was removed from the glass slide, and the barcode-patterned DNA was cross-linked to the glass surface by thermal treatment at 80 °C for 4 hours.

Immunofluorescence staining. Captured tumor cells on the herringbone chips were fixed with 4% paraformaldehyde and subsequently permeabilized with 0.2% Triton X-100 in 1% BSA, all in PBS. Cells were immunostained with phycoerythrin (PE)-conjugated anti-pan cytokeratin (CK) and FITC-conjugated anti-CD45 (BD Biosciences, USA) overnight at 4 °C and washed twice with PBS before imaging. Nuclei were stained with DAPI (Sigma-Aldrich, USA).

System characterization. 1 mL of whole blood sample from healthy donor spiked with EpCAM-positive HCT116 cells was employed as the model system to characterize the integrated microfluidic system. See Supplementary Methods for details.

Sample preparation and clinical sample measurement. Blood samples were obtained from healthy donors and metastatic lung cancer patients in Ruijin Hospital and Shanghai Municipal Hospital of Traditional Chinese Medicine with informed consent. The clinical sample collection was carried out in accordance with the guidelines and protocols approved by the Ethics and Scientific Committees of both institutions. A total of 10 blood samples (4 from lung cancer patients and 6 from healthy donors) were obtained at the middle of vein puncture after first 3 mL of blood was discarded. All blood samples (4 mL taken from patients, and 2 mL taken from healthy donors) were collected into EDTA-contained vacutainer tubes and were processed within 6 h. A volume of 4 mL peripheral blood from patients was equally divided into two parts for CTC enumeration and single-cell secretion profiling. CTCs were captured via a cocktail of photocleavable ssDNA-antibody conjugates (PC-M⁺-EpCAM, PC-M⁺-EGFR, PC-M⁺-HER2 and PC-M⁺-CD44) and a herringbone chip with a 400 μm-long microvortex-generating channel. All steps were as same as described in proof-of-concept experiments. See Supplementary Methods for details.

1. Yu, M., Stott, S., Toner, M., Maheswaran, S. & Haber, D. A. Circulating tumor cells: approaches to isolation and characterization. *J. Cell Biol.* **192**, 373–382 (2011).
2. den Toonder, J. Circulating tumor cells: the Grand Challenge. *Lab Chip* **2011**, **11**, 375–377 (2011).
3. Chaffer, C. L. & Weinberg, R. A. A Perspective on Cancer Cell Metastasis. *Science* **311**, 1559–1564 (2011).
4. Braun, S. *et al.* A pooled analysis of bone marrow micrometastasis in breast cancer. *N. Engl. J. Med.* **353**, 793–802 (2005).

5. Méhes, G., Witt, A., Kubista, E. & Ambros, P. F. Circulating breast cancer cells are frequently apoptotic. *Am. J. Pathol.* **159**, 17–20 (2001).
6. Larson, C. J. *et al.* Apoptosis of circulating tumor cells in prostate cancer patients. *Cytometry A*. **62**, 46–53 (2004).
7. Chambers, A. F., Groom, A. C. & MacDonald, I. C. Dissemination and growth of cancer cells in metastatic sites. *Nat. Rev. Cancer* **2**, 563–572 (2002).
8. Zhang, L. X. *et al.* The Identification and Characterization of Breast Cancer CTCs Competent for Brain Metastasis. *Sci. Transl. Med.* **5**, 189er5 (2013).
9. Baccelli, I. *et al.* Identification of a population of blood circulating tumor cells from breast cancer patients that initiates metastasis in a xenograft assay. *Nat. Biotechnol.* **31**, 539–U143 (2013).
10. Stott, S. L. *et al.* Isolation of circulating tumor cells using a microvortex-generating herringbone-chip. *Proc. Natl. Acad. Sci. U.S.A.* **107**, 18392–18397 (2010).
11. Wang, S. T. *et al.* Highly Efficient Capture of Circulating Tumor Cells by Using Nanostructured Silicon Substrates with Integrated Chaotic Micromixers. *Angew. Chem. Int. Ed.* **2011**, **50**, 3084–3088 (2011).
12. Zhang, N. G. *et al.* Electrospun TiO₂ Nanofiber-Based Cell Capture Assay for Detecting Circulating Tumor Cells from Colorectal and Gastric Cancer Patients. *Adv. Mater.* **24**, 2756–2760 (2012).
13. Hou, H. W. *et al.* Isolation and retrieval of circulating tumor cells using centrifugal forces. *Sci. Rep.* **3**, 1259 (2013).
14. Sun, J. S. *et al.* Double spiral microchannel for label-free tumor cell separation and enrichment. *Lab Chip* **12**, 3952–3960 (2012).
15. Warkiani, M. E. *et al.* Slanted spiral microfluidics for the ultra-fast, label-free isolation of circulating tumor cells. *Lab Chip* **2014**, **14**, 128–137 (2014).
16. Hoshino, K. *et al.* Microchip-based immunomagnetic detection of circulating tumor cells. *Lab Chip* **11**, 3449–3457 (2011).
17. Ozkumur, E. *et al.* Inertial Focusing for Tumor Antigen-Dependent and -Independent Sorting of Rare Circulating Tumor Cells. *Sci. Transl. Med.* **2013**, **5**, 179ra47 (2013).
18. Dalerba, P. *et al.* Single-cell dissection of transcriptional heterogeneity in human colon tumors. *Nat. Biotechnol.* **29**, 1120–U11 (2011).
19. Ramskold, D. *et al.* Full-length mRNA-Seq from single-cell levels of RNA and individual circulating tumor cells. *Nat. Biotechnol.* **30**, 777–782 (2012).
20. Yu, M. *et al.* RNA sequencing of pancreatic circulating tumour cells implicates WNT signalling in metastasis. *Nature* **487**, 510–U130 (2012).
21. Ni, X. H. *et al.* Reproducible copy number variation patterns among single circulating tumor cells of lung cancer patients. *Proc. Natl. Acad. Sci. U.S.A.* **110**, 21083–21088 (2013).
22. Ma, C. *et al.* Multifunctional T-cell Analyses to Study Response and Progression in Adoptive Cell Transfer Immunotherapy. *Cancer Discov.* **3**, 418–429 (2013).
23. Huh, S. J., Liang, S. L., Sharma, A., Dong, C. & Robertson, G. P. Transiently Entrapped Circulating Tumor Cells Interact with Neutrophils to Facilitate Lung Metastasis Development. *Cancer Res.* **70**, 6071–6082 (2010).
24. Alix-Panabieres, C. *et al.* Characterization and enumeration of cells secreting tumor markers in the peripheral blood of breast cancer patients. *J. Immunol. Methods* **299**, 177–188 (2005).
25. Ma, C. *et al.* A clinical microchip for evaluation of single immune cells reveals high functional heterogeneity in phenotypically similar T cells. *Nat. Med.* **17**, 738–U133 (2011).
26. Shi, Q. H. *et al.* Single-cell proteomic chip for profiling intracellular signaling pathways in single tumor cells. *Proc. Natl. Acad. Sci. U. S. A.* **109**, 419–424 (2012).
27. Wei, W. *et al.* Hypoxia induces a phase transition within a kinase signaling network in cancer cells. *Proc. Natl. Acad. Sci. U. S. A.* **110**, E1352–E1360 (2013).
28. Lu, Y. *et al.* High-Throughput Secretomic Analysis of Single Cells to Assess Functional Cellular Heterogeneity. *Anal. Chem.* **85**, 2548–2556 (2013).
29. Stephan, J. P., Schanz, S., Wong, A., Schow, P. & Wong, W. L. T. Development of a frozen cell array as a high-throughput approach for cell-based analysis. *Am. J. Pathology* **161**, 787–797 (2002).
30. Kwong, G. A. *et al.* Modular Nucleic Acid Assembled p/MHC Microarrays for Multiplexed Sorting of Antigen-Specific T Cells. *J. Am. Chem. Soc.* **131**, 9695–9703 (2009).
31. Vermesh, U. *et al.* High-Density, Multiplexed Patterning of Cells at Single-Cell Resolution for Tissue Engineering and Other Applications. *Angew. Chem. Int. Ed.* **50**, 7378–7380 (2011).
32. Finn, F. M., Titus, G., Montibeller, J. A. & Hofmann, K. Hormone-receptor studies with avidin and biotinylinsulin-avidin complexes. *J. Biol. Chem.* **255**, 5742–5746 (1980).
33. Dharmasiri, U. *et al.* High-Throughput Selection, Enumeration, Electrokinetic Manipulation, and Molecular Profiling of Low-Abundance Circulating Tumor Cells Using a Microfluidic System. *Anal. Chem.* **83**, 2301–2309 (2011).
34. Sheng, W., Ogunwobi, O. O., Chen, T., Zhang, J. L. & George, T. J. Capture, release and culture of circulating tumor cells from pancreatic cancer patients using an enhanced mixing chip. *Lab Chip* **14**, 89–98 (2014).
35. Hou, S. *et al.* Capture and Stimulated Release of Circulating Tumor Cells on Polymer-Grafted Silicon Nanostructures. *Adv. Mater.* **11**, 1547–1551 (2013).
36. Shen, Q. L. *et al.* Specific Capture and Release of Circulating Tumor Cells Using Aptamer-Modified Nanosubstrates. *Adv. Mater.* **25**, 2368–2373 (2013).
37. Agasti, S. S., Liang, M., Peterson, V. M., Lee, H. & Weissleder, R. Photocleavable DNA Barcode-Antibody Conjugates Allow Sensitive and Multiplexed Protein Analysis in Single Cells. *J. Am. Chem. Soc.* **134**, 18499–18502 (2012).



38. Ariyasu, S. *et al.* Selective Capture and Collection of Live Target Cells Using a Photoreactive Silicon Wafer Device Modified with Antibodies via a Photocleavable Linker. *Langmuir* **28**, 13118–13126 (2012).
39. Tan, S. J., Yobas, L., Lee, G. Y., Ong, C. N. & Lim, C. T. Microdevice for the isolation and enumeration of cancer cells from blood. *Biomed. Microdevices* **11**, 883–892 (2009).
40. Hosokawa, M. *et al.* Size-Selective Microcavity Array for Rapid and Efficient Detection of Circulating Tumor Cells. *Anal. Chem.* **82**, 6629–6635 (2010).
41. Dalerba, P. *et al.* Phenotypic characterization of human colorectal cancer stem cells. *Proc. Natl. Acad. Sci. U.S.A.* **104**, 10158–10163 (2007).
42. De Larco, J. E. *et al.* A potential role for interleukin-8 in the metastatic phenotype of breast carcinoma cells. *Am J Pathol.* **158**, 639 (2001).
43. Kuramochi, H. *et al.* Vascular endothelial growth factor messenger RNA expression level is preserved in liver metastases compared with corresponding primary colorectal cancer. *Clin Cancer Res.* **12**, 29–33 (2006).
44. Yu, J. *et al.* Microfluidics-Based Single-Cell Functional Proteomics for Fundamental and Applied Biomedical Applications. *Ann. Rev. Anal. Chem.* **7**, 17.1–17.21 (2014).
45. Wei, W. *et al.* Microchip platforms for multiplex single-cell functional proteomics with applications to immunology and cancer research. *Genome Med.* **5**, 75 (2013).
46. Kallergi, G. *et al.* Phosphorylated EGFR and PI3K/Akt signaling kinases are expressed in circulating tumor cells of breast cancer patients. *Breast Cancer Res.* **10**, R80 (2008).

Acknowledgments

The research was supported by National Natural Science Foundation of China (Grant No. 21205077) and Specialized Research Fund for the Doctoral Program of Higher Education (Grant No. 20120073120089, No.20130073120106). Q. H. S. is sponsored by Shanghai Pujiang Program (Grant No. 12PJ1404500) and Youth Program of the National 1000

Talents Project. W. W. is sponsored by National Cancer Institute (Grant No. 5U54CA151819) and Phelps Family Foundation.

Author contributions

Q.H.S. and Y.L.D. designed research. B.Q.Y., B.L.L. and Y.L. contributed clinical samples. D.Y.L. and Z.H.W. performed CTC isolation from patient blood samples. Y.Z. performed single-cell experiments on isolated CTCs from model cell lines and patients. Y.Z., S.S., and M.J.W. performed system characterization based on model cell lines. Q.H.S. and Y.L.D. analyzed the data. Q.H.S., D.M.C., and W.W. wrote the manuscript. All authors reviewed the manuscript.

Additional information

Supplementary information accompanies this paper at <http://www.nature.com/scientificreports>

Competing financial interests: Q.H.S., Y.L.D., Y.Z. and S.S. have filed a patent application on the technology described here.

How to cite this article: Deng, Y. *et al.* An Integrated Microfluidic Chip System for Single-Cell Secretion Profiling of Rare Circulating Tumor Cells. *Sci. Rep.* **4**, 7499; DOI:10.1038/srep07499 (2014).



This work is licensed under a Creative Commons Attribution-NonCommercial-ShareAlike 4.0 International License. The images or other third party material in this article are included in the article's Creative Commons license, unless indicated otherwise in the credit line; if the material is not included under the Creative Commons license, users will need to obtain permission from the license holder in order to reproduce the material. To view a copy of this license, visit <http://creativecommons.org/licenses/by-nc-sa/4.0/>